Proceedings of ERAD (2004): 144–149 © Copernicus GmbH 2004

ERAD 2004

Mapping clouds and precipitation with CloudSat and the afternoon A-Train

T. S. L'Ecuyer, G. L. Stephens, and R. T. Austin

Colorado State University, Fort Collins, Colorado, USA

1 Introduction

Clouds play an important role in many aspects of the Earth's climate system. They provide dynamic reservoirs for liquid and ice in the atmospheric branch of the hydrologic cycle, exert a significant impact on global energy balance, and represent an important factor impacting climate variability. To date, however, the total mass of water that resides in the form of clouds, the spatial and temporal distribution of cloud radiative properties, and the magnitude of potential cloud feedbacks on the general circulation have been difficult to quantify, in part due to a lack of vertically-resolved cloud microphysical property observations on global scales. The CloudSat Cloud Profiling Radar (CPR), the first millimeter wavelength radar to be flown in space, in concert with other sensors aboard the A-Train satellites seeks to provide the first global survey of cloud vertical structure and its variability on synoptic and seasonal timescales providing a unique opportunity to learn more about the role clouds may play in global climate change.

This paper provides an overview of the CloudSat mission and its role as a component of the multi-satellite, multi-sensor A-Train constellation. The estimation-based inversion framework that forms the basis of many of CloudSat's cloud microphysical property and light precipitation retrieval algorithms will be described and examples of the application of two such algorithms to airborne and ground-based cloud radar observations are presented. The last section outlines CloudSat's validation requirements and current plans for achieving them using ground-based and airborne radar observations.

2 The CloudSat mission and the A-Train

Shortly following its launch in April 2004, CloudSat will join Cloud-Aerosol Lidar and Infrared Pathfinder Satellite Observations (CALIPSO) and Aqua in a sun-synchronous orbit at an altitude of 705 km. These satellites and three others: Polarization and Anisotropy of Reflectances for Atmospheric Science coupled with Observations from a Lidar (PARASOL), Aura, and the Orbiting Carbon Observatory (OCO) will ultimately fly in formation providing an unprecidented view of our atmosphere. Fig. 1 presents a conceptual diagram of this constellation, nicknamed the "A-Train" after its lead member, Aqua. Also provided are the approximate equatorial crossing times for each satellite indicating their separation along the orbit. Until the launch of OCO in the more distant future, Aqua will lead the A-Train carrying a variety of instruments for measuring the global distribution of water in all of its phases such as the Moderate Resolution Imaging Spectroradiometer (MODIS) and Advanced Microwave Scanning Radiometer (AMSR) for observing clouds and precipitation, respectively. Aqua also carries a Clouds and the Earth's Radiant Energy System (CERES) instrument for measuring top of the atmosphere fluxes. CloudSat and CALIPSO will fly in a tight formation with one another closely following Aqua. Each carries an active sensor for measuring vertical profiles of clouds and aerosols. The next satellite, PARASOL, will provide polarized radiance measurements of clouds and aerosols. Aura follows PARASOL with a payload devoted to determining the horizontal and vertical distributions of atmospheric pollutants and greenhouse gases. In the more distant future, the OCO satellite is expected to launch and join the front of the A-Train providing measurements of the global distribution of CO_2.

The over-arching goal of the A-Train constellation is to provide a synergistic view of the primary components of the global hydrologic cycle and energy budget including water vapor, clouds, rainfall, aerosols, and the distribution of various chemical species in the atmosphere as well as longwave and shortwave radiative fluxes at the top of the atmosphere. At an orbit inclination of 98.2°, the A-Train observations will provide a dataset with which to study the interaction of these quantities on a global scale. CloudSat's role in the A-Train

Correspondence to: T. S. L'Ecuyer
(tristan@atmos.colostate.edu)

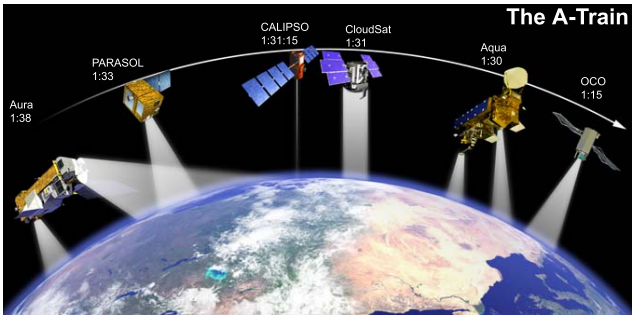

Fig. 1. Conceptual diagram of the proposed A-Train constellation.

concept is to provide vertical cross-sections of cloud liquid and ice water content and particle size by flying the first millimeter wavelength cloud radar in space (Stephens et al., 2002). The Cloud Profiling Radar (CPR) aboard CloudSat is a 94 GHz (3 mm) nadir-viewing radar with 500 m vertical resolution. At its altitude of 705 km, the CPR will provide vertical profiles of radar reflectivity down to −26 dBZ at a spatial resolution of ∼1.5 km. The cloud and precipitation products derived from these observations will offer insight into processes of fundamental importance to understanding the role of clouds in the large-scale environment. These products, in combination with those from other A-Train sensors, have the potential to both improve our ability to predict the weather and advance our understanding of key climatic processes.

3 Remote Sensing Philosophy and Products

The suite of algorithms developed for CloudSat have been designed to combine the CPR observations with complementary information from the other sensors across the A-Train, such as AMSR-E and MODIS radiance data from Aqua, to measure vertical distributions of liquid and ice water content in the atmosphere. Table 1 summarizes CloudSat's level-2 standard and experimental data products. The first two products make use of CPR reflectivities to establish the cloud geometric profile and identify cloud type including a discrimination of cloud phase based on cloud height, geometric thickness, and the strength of the observed reflectivities. The observations are subsequently employed to retrieve profiles of cloud liquid and ice water content where appropriate. These cloud properties are then combined with properties of the background atmosphere and surface from European Centre for Medium Range Weather Forecasts (ECMWF) analyses to simulate upwelling and downwelling radiative fluxes and heating rates through the atmospheric column making it possible to study connections between clouds and the Earth's radiation budget.

In addition to these standard products, a number of experimental algorithms have being developed directed toward extracting the maximum information possible from the CPR observations. In addition to total column optical depth and cloud layer-averaged particle size, it is anticipated that CloudSat will be capable of detecting rainfall and snow. Due to its enhanced sensitivity over lower frequency radars, the CPR is well-suited to retrieving light liquid precipitation, including drizzle, and identifying falling snow. Such products are expected to supplement the standard cloud products helping put them into the larger context of the global hydrologic cycle. The combination of cloud liquid water content and light precipitation products, for example, may provide insight into the mechanisms that govern the transition from cloud to precipitation.

CloudSat is also dedicated to supplying rigorously-derived estimates of the uncertainties in each product. As a result, many of its algorithms have been formulated using the optimal estimation methodology (Rodgers, 2000). Within this framework, the most probable set of retrieval parameters is determined by minimizing the difference between a set of simulated measurements and observations subject to a desired set of a priori and observational constraints

$$\Phi = (\mathbf{x}-\mathbf{x}_a)^T\mathbf{S}_a^{-1}(\mathbf{x}-\mathbf{x}_a) + (\mathbf{y}-F(\mathbf{x}))^T \times \mathbf{S}_y^{-1}(\mathbf{y}-F(\mathbf{x})) + C\left[\left(\sum \mathbf{x} - Z\right), \sigma_Z\right] \quad (1)$$

where $\mathbf{y}$ represents the vector of observed reflectivities, $\mathbf{x}$ is the vector of microphysical properties to be retrieved, and $\mathbf{x}_a$ is an appropriate initial or *a priori* guess at the expected value of $\mathbf{x}$. $F(\mathbf{x})$ is a set of simulated reflectivities using our best understanding of the underlying physics relating the retrieval parameters to the observations. Z represents an integral constraint such as column optical depth in the case of cloud retrievals or path-integrated attenuation (PIA) for precipitation retrievals.

Among the benefits of adopting the optimal estimation formalism is that it allows the formal inclusion of different forms of information including measurements from multiple sensors as well as a priori knowledge of the retrieval parameters. In addition, the technique provides a mechanism for explicitly specifying the uncertainties in all input data and assumptions in the forward model (through the $\mathbf{S}_y$ and $\mathbf{S}_a$ matrices) weighting each piece of information accordingly. Finally, the technique provides a mathematical framework for propagating each of these individual sources of error through the retrieval to yield quantitative measures of the uncertainty in each retrieval parameter. Specifically, the algorithms provide a retrieval error covariance matrix of the form:

$$\mathbf{S}_x = \left[\mathbf{S}_a^{-1} + \mathbf{K}^T\mathbf{S}_y^{-1}\mathbf{K} + \frac{\mathbf{L}^T\mathbf{L}}{\sigma_Z^2}\right]^{-1} \quad (2)$$

where the vector $\mathbf{L}$ consists of the derivatives of the constraint, Z, with respect to each retrieval parameter and the matrix $\mathbf{K}$ is the Jacobian of the forward model with respect to the retrieval vector, with elements given by $K_{ij} = \partial F_i/\partial x_j$.

Table 1. CloudSat's level-2 standard and experimental data products.

Product	Resolution (Accuracy)	Description
	Standard Products	
Cloud Mask	500 m (N/A)	Cloud geometric distribution
Cloud Classification	N/A (N/A)	Cloud type identification
Cloud Ice Water Content	500 m (30–50%)	Vertical profile of cloud ice water content
Cloud Liquid Water Content	500 m (30–50%)	Vertical profile of cloud liquid water content
Fluxes	500 m (10 Wm^{-2})	Broadband radiative fluxes
Heating rates	500 m (1 K d^{-1})	Broadband radiative heating rates
	Experimental Products	
Precipitation Occurrence	500 m (N/A)	Liquid and solid precipitation identification
Path-integrated Attenuation	TBD (TBD)	Surface return-based radar attenuation estimate
Rainfall rate	TBD (TBD)	Rainfall rate for light liquid precipitation
Cloud optical depth	Cloud layer (TBD)	CPR+MODIS-based estimate of cloud optical depth
Particle size	Cloud layer (TBD)	Cloud droplet/particle effective radius

4 Liquid Cloud and Precipitation Algorithms

Austin and Stephens (2001) describe an algorithm for retrieving liquid cloud microphysical properties from CPR reflectivity measurements constrained by visible optical depth from coincident passive observations. The approach, built in the optimal estimation framework, assumes a log-normal distribution of cloud droplets

$$N(r) = \frac{N_T}{\sqrt{2\pi}\sigma_{log} r} exp\left[\frac{-\ln^2(r/r_g)}{2\sigma_{log}^2}\right] \quad (3)$$

to retrieve the vertical profile of geometric mean radius, $r_g(z)$, column-mean number concentration, N_T, and column-mean geometric standard deviation, $\sigma_g = e^{\sigma_{log}}$. Referring to Eq. (1), the *a priori* values of these quantities and their uncertainties, $\mathbf{S}_a$, derive from the climatology of *in situ* observations of low-level stratiform clouds made between 1972 and 1995 presented in Miles et al. (2000). The measurement vector, **y**, consists of the observed profile of CPR reflectivities while the constraint enters in the form of a visible optical depth derived from co-located MODIS radiance data. Appropriate uncertainties for each are determined through analysis of the sensitivities of the radar and radiative transfer forward models to assumptions such as the shape of the assumed drop size distribution and ambient temperature and humidity profiles.

Figure 2 presents an example of the inputs to the Austin and Stephens (2001) algorithm obtained at the Atmospheric Radiation Measurement (ARM) site in Oklahoma. Radar reflectivities, in this case from the Millimeter-wave Cloud Radar (MMCR), are combined with visible optical depth information inferred from the Multi-Filter Rotating Shadowband Radiometer (MFRSR) to retrieve profiles of liquid water content and effective radius presented in the top panels of Fig. 3. While these instruments do not correspond exactly to those aboard CloudSat and Aqua, they provide a reasonable approximation to the CPR/MODIS combination to which the algorithm will ultimately be applied.

Effective radii range from 4.5 μm at cloud base to 6.5 μm near cloud top while liquid water contents range from less than 0.2 gm^{-3} at cloud base to 0.45 gm^{-3} near cloud top. The last two panels illustrate the expected uncertainties in liquid water content and liquid water path, respectively, owing to the combination of measurement, model, and a priori errors. In both cases uncertainties are between 5 and 10% across the full five hour time-series.

CloudSat's experimental light liquid precipitation algorithm is constructed using a similar technique (L'Ecuyer and Stephens, 2002). Due to the strong attenuation of precipitation-sized hydrometeors at 94 GHz, however, an integral constraint in the form of either PIA or precipitation water path (PWP) is required to unambigously retrieve rainrate. The top panel of Fig. 4 presents Airborne Cloud Radar (ACR) data obtained from a single flight leg during the Advanced Microwave Scanning Radiometer (AMSR) validation experiment that took place in Wakasa Bay, Japan in January and February, 2003.

The scene consists of a thick precipitating cirrus cloud overlying a persistent area of light rainfall indicated by a well-defined melting level at ~1.8 km. Reflectivities exceeding 10 dBZ throughout most of the scene indicate the presence of large precipitating liquid and ice particles and the decrease in reflectivity in the rainfall between the melting level and the surface is indicative of their strong attenuation at 94 GHz. The remainder of Fig. 4 presents estimates of the PIA and melting level within the scene.

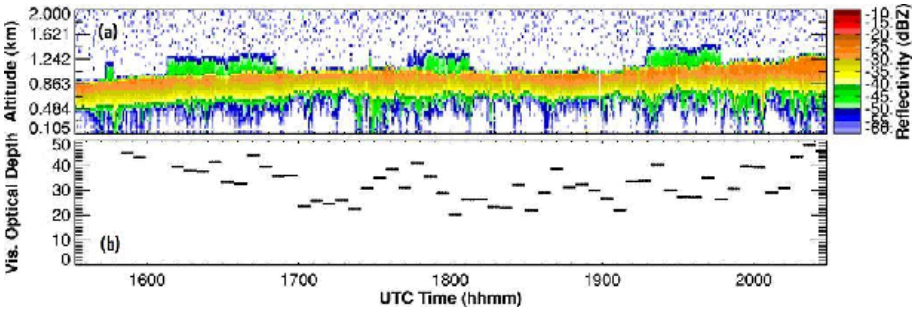

Fig. 2. MMCR and MFRSR observations of a liquid cloud at the ARM CART site in Oklahoma.

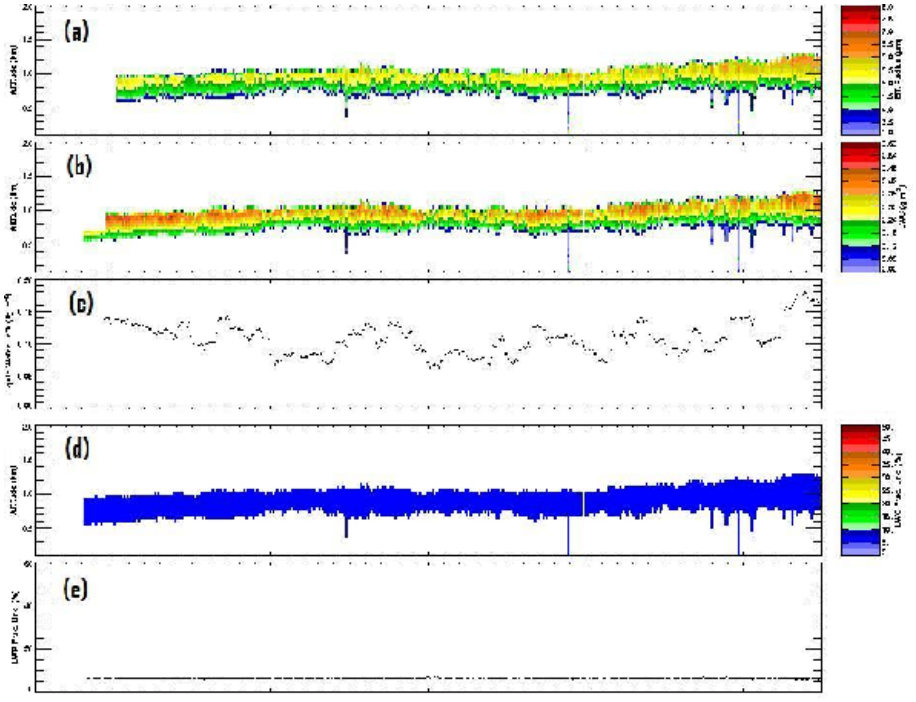

Fig. 3. Retieval results for the example presented in Fig. 2. Effective radius and liquid water content and are presented in panels (a) and (b), respectively. Liquid water content is integrated in the vertical to provide liquid water path in panel (c). Associated uncertainties in the LWC and LWP estimates are presented in panels (d) and (e), respectively.

The algorithm proceeds by creating an initial profile of liquid and ice water content using Z-IWC and Z-LWC relationships and accounting for attenuation via corresponding k-Z relationships in a manner analogous to that of Hitschfeld and Borden (1954). Below the melting level, hydrometeors are assumed to follow a Marshall-Palmer (Marshall and Palmer, 1948) distribution of spherical liquid drops while those above are assumed to follow an equivalent distribution of ice spheres. The retrieval then iteratively minimizes Eq. (1) using this initial profile for $\mathbf{x}_a$ and the PIA estimate as a constraint. Mie theory is used to compute reflectivities and appropriate attenuation corrections for each layer to compare to the observed reflectivities in subsequent iterations.

Retrieved profiles of liquid and ice water content and surface rainfall rate for this case are presented in Fig. 5. Retrieved rainrates are typically less than $1\,\mathrm{mm\,h^{-1}}$ across much of the flight line with the exception of a three more intense rain shafts near the end of the leg. The corresponding PIA values range from 15–25 dB in these regions confirming the presence of more intense precipitation there (and constraining the retrieval accordingly). Fractional uncertainties in these quantities due to reflectivity and PIA measurement errors and uncertainties in assumed drop size distribution (DSD) are presented in the second and lowest panels.

5 Validation

Central to the optimal estimation approach that forms the basis of CloudSat's microphysical property algorithms are the uncertainties in the forward model assumptions. In addition to measurement errors, uncertaintiess in any parameter required to model the observations that is not explicitly

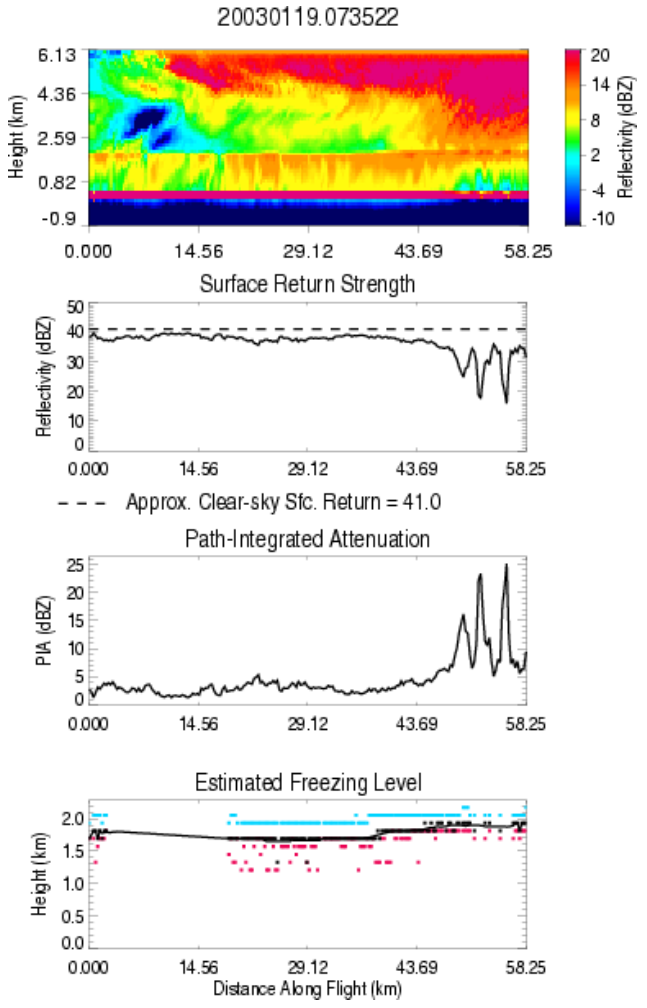

Fig. 4. Observations of light rainfall from the Wakasa Bay field experiment. The top panel presents observed reflectivities at 94 GHz. The second and third panels illustrate the method for deriving PIA based on the difference between the observed strength of the surface return (solid line) and an estimate of its strength under clear-sky conditions (dashed line). The lowest panel presents the estimated melting level determined from the vertical gradient of the observed reflectivity field.

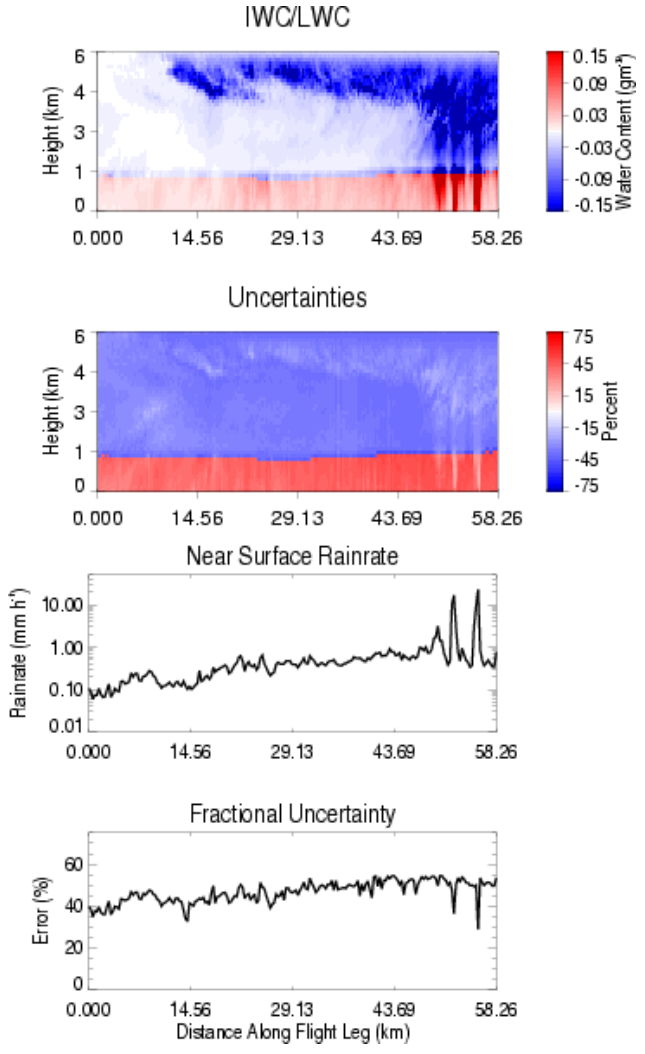

Fig. 5. Results of the application of CloudSat's experimental precipitation algorithm to the case presented in Fig. 4. The upper two panels present retrieved liquid and ice water content and their uncertainties, respectively (note quantities pertaining to ice have been plotted as negative values to improve contrast). Retrieved near surface rainfall rate and its uncertainty are presented in the lowest two panels, respectively.

retrieved must be accounted for in the measurement and model error covariance matrix. It is clear rom Eq. (1) that $\mathbf{S}_y$ and $\mathbf{S}_a$ dictate the amplitude with which to weight the observations and *a priori* information used in the retrieval and, ultimately, determine the uncertainty characteristics of the products. As a result, CloudSat's validation strategy relies on a combination of traditional correlative analysis of its products against ground truth as well as analysis of the individual component assumptions that comprise each algorithm in an effort to verify these covariance assumptions.

To this end, planned validation activities for CloudSat involve merging data from a variety of sources including in-situ ground and aircraft observations and co-located remote observations from ground-based and airborne radars in order to study all aspects of the retrieval problem. Such datasets offer the potential for a complete, end-to-end, evaluation of retrieval algorithms including the following:

– establishing bounds on the a priori information used to initialize the algorithms such as cloud liquid water path;

– confirming the theoretical relationships between the measurements and retrieval parameters through coincident observations of microphysical properties and the radiance and reflectivity fields they produce;

– testing the assumptions required to model the radiative transfer through the atmosphere and clouds such as assumed DSD, crystal habit, and humidity profiles;

– evaluating the resulting cloud microphysical property and rainfall products using ground truth to confirm the associated estimates of retrieval error.

This strategy does not require all validation data to be directly associated with coincident satellite overpasses allowing the use of systematic observations from continously-operated sites and archived data from field campaigns that concluded prior to launch in many aspects of validation.

Due to the nearly global coverage of the A-Train orbit, comprehensive validation of CloudSat's products requires measurements in a variety of locations and seasons in order to span the wide range of cloud and precipitation regimes that occur in nature. As a result, it is anticipated that a majority (if not all) of the CloudSat validation activities will be coordinated with larger field programs that seek to better understand clouds and precipitation and improve their representation in models. In addition, CloudSat will benefit greatly from the regular ground-based and aircraft measurement activities ongoing at major atmospheric measurement sites and universities within the United States, Japan, and Europe. European sites such as the Cabauw Experimental Site for Atmospheric Research (CESAR) and the Baltic Radar Network (BALTRAD) may play in an important role CloudSat's validation strategy through their year-round observations of mid to high latitude cloud and precipitation systems.

References

Austin, R. T. and Stephens, G. L.: Retrieval of stratus cloud microphysical parameters using millimeter-wave radar and visible optical depth in preparation for CloudSat. Part I: Algorithm formulation, J. Geophys. Res., 106, 28 233–28 242, 2001.

Hitschfeld, W. and Borden, J.: Errors inherent in the radar measurement of rainfall at attenuating wavelengths, J. Appl. Meteor., 11, 58–67, 1954.

L'Ecuyer, T. S. and Stephens, G. L.: An estimation-based precipitation retrieval algorithm for attenuating radars, J. Appl. Meteor., 41, 272–285, 2002.

Marshall, J. S. and Palmer, W. H.: The distribution of raindrops with size, J. Meteor., 5, 165–166, 1948.

Miles, N. L., Verlinde, J., and Clothiaux, E. E.: Cloud droplet size distributions in low-level stratiform clouds, J. Atmos. Sci, 57, 295–311, 2000.

Rodgers, C. D.: Inverse Methods for Atmospheric Sounding. Theory and Practice, World Scientific, Singapore, 2000.

Stephens, G. L., Vane, D. G., Boain, R. J., Mace, G. G., Sassen, K., Wang, Z., Illingworth, A. J., O'Connor, E. J., Rossow, W. B., Durden, S. L., Miller, S. D., Austin, R. T., Benedetti, A., Mitrescu, C., and Team, T. C. S.: The CloudSat mission and the A-Train: A new dimension of space-based observations of clouds and precipitation, Bull. Amer. Meteor. Soc., 83, 1771–1790, 2002.